Ionization and charge transfer of atomic hydrogen in collision with multiply charged ions

Nobuyuki Toshima
Institute of Applied Physics, University of Tsukuba, Tsukuba, Ibaraki 305, Japan
and Institute of Physical and Chemical Research (RIKEN), Wako 351-01, Japan
(Received 5 July 1994)

Ionization and charge-transfer cross sections of atomic hydrogen in collision with multiply charged ions are calculated for various projectile charges ($Z = 2$–8) in the energy range from 1 to 400 keV/amu by the atomic-orbital close-coupling method. Many pseudostates constructed from Gaussian-type orbitals are used on the projectile and the target for the representation of continuum states. The present ionization cross sections show systematic agreement with measurements for He^{2+}, Li^{3+}, and C^{6+} impact over the entire energy range where experimental data are available. The present calculations also produce reliable consistent cross sections for excitation and electron capture simultaneously.

PACS number(s): 34.50.Fa, 34.70.+e

I. INTRODUCTION

The close-coupling method has been widely used in various fields of atomic collision physics with the recognition that it is one of the most reliable and powerful theoretical approaches. It is mostly applied to scattering processes in the intermediate- or low-energy region, where the multiple scattering effect is so significant that perturbative approaches are not applicable.

For ion-atom collisions, the description can be simplified by the adoption of the semiclassical version based on the impact-parameter method unless the collision energy is extremely low. Even under this simplification, solving the coupled equations is very time consuming because of the two-center nature of the coupling matrix elements. Nevertheless, the size of coupled equations tends to be increased for the improvement of the convergence owing to the recent progress of high-speed computers. Although good agreement has been achieved with experimental data for various excitation and electron capture processes, extensive study of ionization processes has not been performed yet. The contribution of the continuum states are usually taken into account through discretized continuum states constructed by the diagonalization of the target and projectile Hamiltonians in terms of a set of square integrable basis functions. The purpose of inclusion of pseudocontinuum states has been in most cases improvement of the description of the two-center nature of the electronic wave functions, and the number of positive-energy pseudostates is not large enough to calculate ionization cross sections directly.

The expansion in terms of atomic orbitals centered around the target and projectile nuclei is adequate in the energy range where the projectile velocity is comparable to that of the relevant bound electron. The Slater-type orbitals have been mostly used for the construction of the basis function of the expansion. The existence of the electron translation factor (ETF), which accounts for the different translational motion of the two nuclei, makes impossible the analytic evaluation of the two-center matrix elements based on the Slater-type orbital expansion. Accurate numerical evaluation of the matrix elements becomes rather difficult when the collision energy is high owing to the rapid oscillation of the ETF or when the states have many nodal structures.

Electron capture processes have a peculiarity that the ordinary first Born approximation does not give the leading contribution even at the high-energy limit. It is well-known that this phenomena is due to the Thomas double scattering mechanism, which was originally predicted by the purely classical mechanics. This mechanism had been studied by many workers using entirely perturbative approaches, namely, the second-order perturbation theory or various types of distorted-wave theories that contain the second-order term in it, until Toshima and Eichler [1] succeeded in showing that the contribution of the double scattering can be identified correctly in the close-coupling calculations for charge transfer. They also showed that the double scatterings are mediated by the high-lying continuum states that have the same velocity component with the relative motion. They have avoided the difficulty in numerical integration of the matrix elements between continuum states by the introduction of the Gaussian-type orbitals (GTO) for the expansion. The GTO representation enables all the two-center matrix elements to be evaluated analytically with any desired accuracy regardless of the collision energy. Toshima [2] later extended the GTO expansion method to the calculation of the perturbation series for charge transfer. It was demonstrated that the GTO representation is a very powerful method for the treatment of the processes in which continuum states play a decisive role.

Most of the existing theoretical calculations of ionization cross sections of atomic hydrogen in collision with multiply charged ions are based on perturbative approaches and their agreement with experimental data is not satisfactory at intermediate- and low-energy regions [3]. Close-coupling calculations show much better

agreement, but they have been done only for ions with small net charges [4,5]. Recently Toshima [6] investigated the ionization process in C^{6+} + H collisions by means of the close-coupling method developed for the study of the Thomas double scattering process stated above. In this study he found that deep bound states of the projectile ion have a significant contribution to the ionization and excitation cross sections below 10 keV and the neglect of those states causes a serious overestimation of the cross sections. Fritsch [7] also executed large-scale close-coupling calculations for the excitation processes in Be^{4+} + H and C^{6+} + H collisions, including all the deep bound states of the projectile ions in the expansion.

In this article we calculate ionization and electron capture cross sections for the collisions of atomic hydrogen with multiply charged naked ions for the nuclear charges $Z = 2 - 8$,

$$A^{Z+} + \mathrm{H}(1s) \rightarrow A^{Z+} + p + e \rightarrow A^{(Z-1)+} + p\,, \quad (1)$$

by means of the close-coupling method.

II. THEORY

The numerical procedure of the present close-coupling method has been shown in details in previous papers [1,6] and we give only a brief remark on it here. The relative motion of the heavy particles is described classically by a rectilinear trajectory with a constant velocity v in the impact-parameter representation. The time-dependent two-center electronic wave function is expanded in a standard way as

$$\Psi(\mathbf{r},t) = \sum_{i=1}^{N_T} a_i(t)\psi_i^T(\mathbf{r}_T,t) + \sum_{i=N_T+1}^{N} a_i(t)\psi_i^P(\mathbf{r}_P,t), \quad (2)$$

where $\psi_i^T(\mathbf{r}_T,t)$ and $\psi_i^P(\mathbf{r}_P,t)$ are the target and the projectile atomic orbital with appropriate electron translation factors attached and $\mathbf{r}_T, \mathbf{r}_P$ are the electron coordinates measured from the target and projectile nucleus, respectively. The eigenfunctions of each center are further expanded in terms of the Gaussian-type basis functions as

$$\varphi_{nlm}(\mathbf{r}) = \sum_{\nu} c_\nu^{(n\ell)}\, e^{-\alpha_\nu r^2}\, r^\ell Y_{\ell m}(\hat{\mathbf{r}}), \quad (3)$$

where the nonlinear parameters α_ν are generated as a modified geometrical progression. The coefficients $c_\nu^{n\ell}$ are determined so as to diagonalize the atomic Hamiltonian of the target and the projectile.

III. RESULTS AND DISCUSSION

The energy levels of the atomic orbitals used for the expansion (2) are listed in Tables I–VIII. We have explicitly coupled deep bound states of multiply charged ions on the projectile following the findings in the preliminary study of the ionization process of C^{6+} + H collisions [6], though the direct transition probabilities to those states are negligibly small. The basis set used for the atomic hydrogen is larger than that used in the preliminary calculations in that the bound states with $n = 3$ and 4 are added. The inclusion of these excited states of H makes the ionization cross sections larger around 100 keV/amu but smaller below 10 keV/amu, while the capture cross sections are changed little.

TABLE I. The eigenvalues (a.u.) of H obtained by diagonalizing the atomic Hamiltonian in terms of Gauss-type basis functions.

$\ell = 0$	$\ell = 1$	$\ell = 2$	$\ell = 3$	$\ell = 4$
-0.500				
-0.125	-0.125			
-0.056	-0.056	-0.056		
-0.031	-0.031	-0.031	-0.031	
0.009	0.004	0.048	0.031	0.016
0.070	0.058	0.177	0.146	0.125
0.208	0.185	0.514	0.494	0.575
0.515	0.480	1.403	1.567	2.536
1.189	1.164	3.795	5.000	11.80
2.657	2.755	10.44		
5.863	6.519			

The numbers of Gaussian-type orbitals used for the expansion of (3) are 20, 16, 13, 11, 10, 8, 7, and 6 for $\ell =$ 0–7, respectively. These numbers and the ranges of the nonlinear parameters α_ν are determined and optimized so as to produce the wave functions of all the bound states in Tables I–VIII sufficiently accurately; the matrix elements among bound states agree with those calculated in terms of exact hydrogenic wave functions within an inaccuracy of 1%. Increasing the Gaussian orbitals still further, the eigenvalues of the pseudocontinuum states shift to lower energies as a whole and the spacings among them become smaller but the calculated ionization cross sections change little. The convergence of capture cross sections is achieved for a smaller number of Gaussian orbitals.

Figure 1 shows the ionization and capture cross sections for He^{2+} + H. The capture cross sections are very

TABLE II. The eigenvalues (a.u.) of He^+ obtained by diagonalizing the atomic Hamiltonian in terms of Gauss-type basis functions.

$\ell = 0$	$\ell = 1$	$\ell = 2$	$\ell = 3$	$\ell = 4$
-2.000				
-0.500	-0.500			
-0.222	-0.222	-0.222		
-0.125	-0.125	-0.125	-0.125	
-0.080	-0.080	-0.080	-0.080	-0.080
0.057	0.059	0.095	0.066	0.128
0.209	0.239	0.412	0.364	0.937
0.517	0.638	1.254	1.255	4.829
1.137	1.505	3.447	3.898	
2.367	3.368			
4.802	7.384			

TABLE III. The eigenvalues (a.u.) of Li^{2+} obtained by diagonalizing the atomic Hamiltonian in terms of Gauss-type basis functions.

$\ell = 0$	$\ell = 1$	$\ell = 2$	$\ell = 3$	$\ell = 4$
-4.499				
-1.125	-1.125			
-0.500	-0.500	-0.500		
-0.281	-0.281	-0.281	-0.281	
-0.180	-0.180	-0.180	-0.180	-0.180
0.096	0.097	0.154	0.112	0.216
0.378	0.415	0.693	0.647	1.614
0.927	1.090	2.061	2.182	7.961
1.990	2.499	5.462	6.541	
4.033	5.414			
7.957				

TABLE IV. The eigenvalues (a.u.) of Be^{3+} obtained by diagonalizing the atomic Hamiltonian in terms of Gauss-type basis functions.

$\ell = 0$	$\ell = 1$	$\ell = 2$	$\ell = 3$	$\ell = 4$
-7.992				
-2.000	-2.000			
-0.889	-0.889	-0.889		
-0.500	-0.500	-0.500	-0.500	
-0.320	-0.320	-0.320	-0.320	-0.320
0.237	0.082	0.053	0.028	0.292
0.904	0.457	1.095	1.243	1.980
2.426	1.282	4.819	6.463	8.592
5.779	3.043	6.767		

TABLE V. The eigenvalues (a.u.) of B^{4+} obtained by diagonalizing the atomic Hamiltonian in terms of Gauss-type basis functions.

$\ell = 0$	$\ell = 1$	$\ell = 2$	$\ell = 3$	$\ell = 4$
-12.49				
-3.123	-3.125			
-1.388	-1.389	-1.389		
-0.781	-0.781	-0.782	-0.781	
-0.500	-0.500	-0.500	-0.500	-0.500
0.371	0.129	0.082	0.044	0.456
1.413	0.715	1.711	1.942	3.093
3.790	2.004	7.530		
9.029	4.755			

TABLE VI. The eigenvalues (a.u.) of C^{5+} obtained by diagonalizing the atomic Hamiltonian in terms of Gaussian-type basis functions.

$\ell = 0$	$\ell = 1$	$\ell = 2$	$\ell = 3$	$\ell = 4$	$\ell = 5$
-17.97					
-4.495	-4.500				
-1.998	-2.000	-2.000			
-1.124	-1.125	-1.125	-1.125		
-0.720	-0.720	-0.720	-0.720	-0.720	
-0.500	-0.500	-0.500	-0.500	-0.500	-0.500
0.252	0.526	0.666	0.626	0.480	0.194
2.106	2.847	3.013	3.037	1.917	
2.770	5.911	8.550			
6.299					

TABLE VII. The eigenvalues (a.u.) of N^{6+} obtained by diagonalizing the atomic Hamiltonian in terms of Gaussian-type basis functions.

$\ell = 0$	$\ell = 1$	$\ell = 2$	$\ell = 3$	$\ell = 4$	$\ell = 5$	$\ell = 6$
-24.49						
-6.123	-6.125					
-2.722	-2.722	-2.722				
-1.531	-1.531	-1.531	-1.531			
-0.980	-0.980	-0.980	-0.980	-0.980		
-0.680	-0.681	-0.681	-0.680	-0.681	-0.681	
-0.500	-0.500	-0.500	-0.500	-0.500	-0.500	-0.500
0.673	0.312	0.319	0.249	0.469	0.281	0.927
3.412	2.237	2.588	2.584	2.559	2.028	4.419
10.85	7.516	9.184	9.907	8.580	8.682	

close to the results of the triple-center close-coupling calculations of Winter [5] but the ionization cross sections are considerably smaller than Winter's results. It is to be noted that the ionization cross sections decrease generally as one increases the number of the basis states at low energies according to the calculations of Winter. We also confirmed this tendency in the present calculations. The ionization cross sections of the adiabatic superpromotion model by Janev, Ivanovski, and Solov'ev [9] are closer to the present results, though their cross sections fail to reproduce the experimental data [10,11] above 20 keV/amu, where the adiabatic representation breaks down. The present ionization cross sections are larger than the measured cross sections by 10–20 % above 100 keV/amu. It needs to be mentioned that the experimental cross sections are normalized to the Born cross section at 1.5 MeV/amu but the close-coupling ionization cross section does not converge to the Born approximation yet even at this energy [12].

Figure 2 gives the cross sections for the process of Li^{3+} + H. The present capture cross sections agree well with other close-coupling results of Fritsch and Lin [13] except above 10 keV/amu. The difference between the two cross sections arises mainly from the contribution of the capture to the $n = 5$ states, which were neglected in their calculations. The agreement of the present ionization cross sections with the experimental data [14] is better than in Fig. 1.

TABLE VIII. The eigenvalues (a.u.) of O^{7+} obtained by diagonalizing the atomic Hamiltonian in terms of Gaussian-type basis functions.

$\ell = 0$	$\ell = 1$	$\ell = 2$	$\ell = 3$	$\ell = 4$	$\ell = 5$	$\ell = 6$	$\ell = 7$
-31.19							
-7.896	-7.980						
-3.525	-3.548	-3.555					
-1.987	-1.997	-2.000	-2.000				
-1.273	-1.278	-1.280	-1.280	-1.279			
-0.885	-0.888	-0.889	-0.889	-0.888	-0.889		
-0.651	-0.652	-0.653	-0.653	-0.652	-0.653	-0.653	
-0.498	-0.500	-0.500	-0.500	-0.499	-0.500	-0.500	-0.500
0.612	0.211	0.541	0.320	0.238	0.009	0.298	0.005
2.607	1.403	2.847	2.312	1.335	1.365		
7.380	4.398	9.113	7.788				

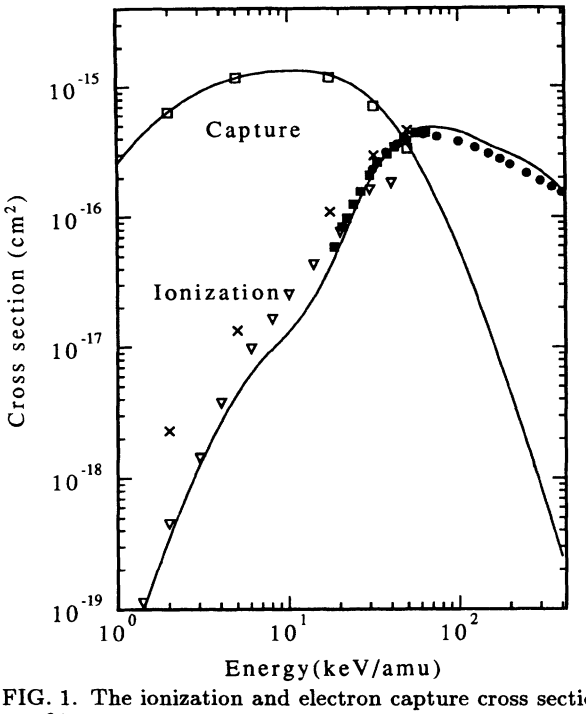

FIG. 1. The ionization and electron capture cross sections for He^{2+} + H(1s). The solid lines are the present calculations. The open squares and the crosses are the three-center close-coupling calculations of Winter [5] and the inverted triangles are the adiabatic superpromotion model of Janev *et al.* [9]. The solid circles and solid squares are the experimental ionization cross sections of Shah and Gilbody [10] and Shah *et al.* [11], respectively.

In Figs. 3 and 4, we present the cross sections for Be^{4+} + H and B^{5+} + H, respectively. The agreement of the capture cross sections with the results of Fritsch and Lin [8] is satisfactory similarly to Fig. 2. No experiment has been done for the measurement of the ionization cross sections. A double-humped structure has appeared in the ionization cross sections at low energies. This structure can be seen commonly in the ionization processes when the nuclear charge Z is large, and it becomes more prominent with increasing Z.

Figure 5 gives the cross sections for C^{6+} + H. This process was studied using a smaller basis set in the preliminary report [6]. Experimental data for the ionization exists only at 400 keV/amu [3]. The present calculations give the cross section of 1.21×10^{-15} cm^2, which is slightly larger than the measured value of $(1.07 \pm 0.06) \times 10^{-15}$ cm^2. Figures 6 and 7 show the cross sections for N^{7+} + H and O^{8+} + H, respectively. In Figs. 5–7, we also compare the capture cross sections with the measurements of Meyer *et al.* [15]. The present capture cross sections are generally larger than the measured values, though the difference is within the uncertainty arising from the experimental errors. The difference between the capture cross sections of the present work and Fritsch and Lin [8] above 10 keV/amu arises from the same reason as in Fig. 2; the capture to highly excited states neglected by them is contributing there. In Fig. 8 we present partial cross sections of the electron capture into each shell for O^{8+} + H(1s) collisions. We see that the neglect of the highly excited states of $n = 7$ and $n = 8$ leads to the underestimate of capture cross sections at E

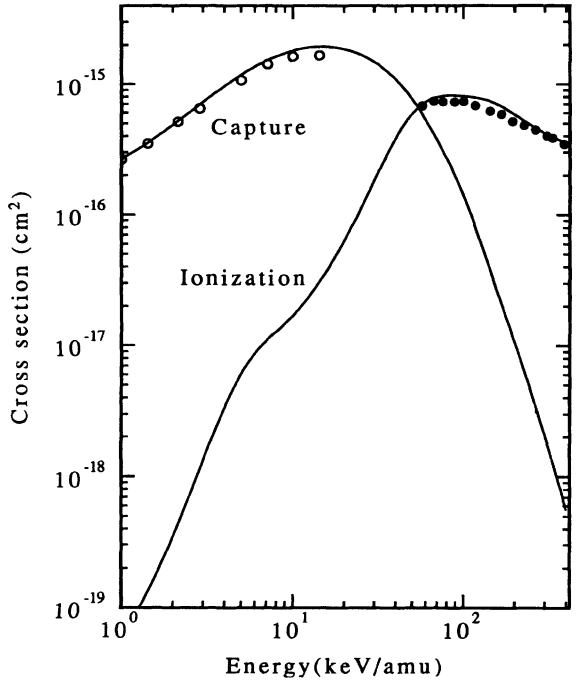

FIG. 2. The ionization and electron capture cross sections for Li^{3+} + H(1s). The solid lines are the present calculations. The open circles are the close-coupling calculations of Fritsch and Lin [13]. The solid circles are the experimental ionization cross sections of Shah and Gilbody [14].

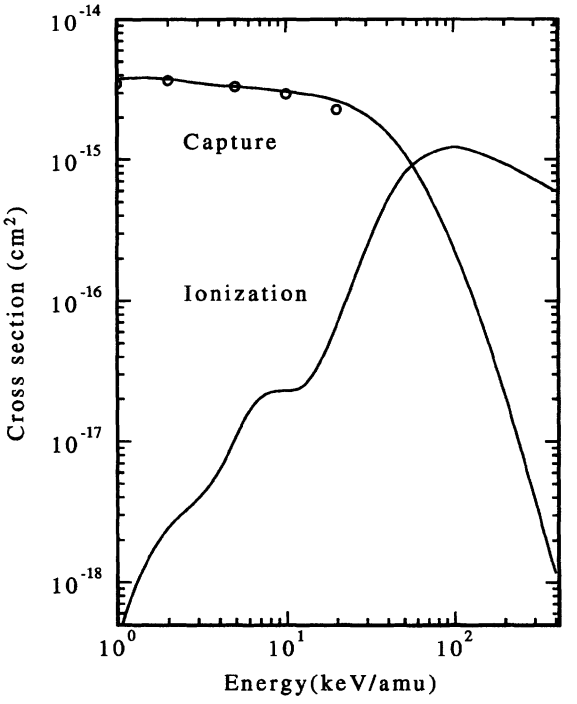

FIG. 3. The ionization and electron capture cross sections for Be^{4+} + H(1s). The open circles are the close-coupling calculations of Fritsch and Lin [8].

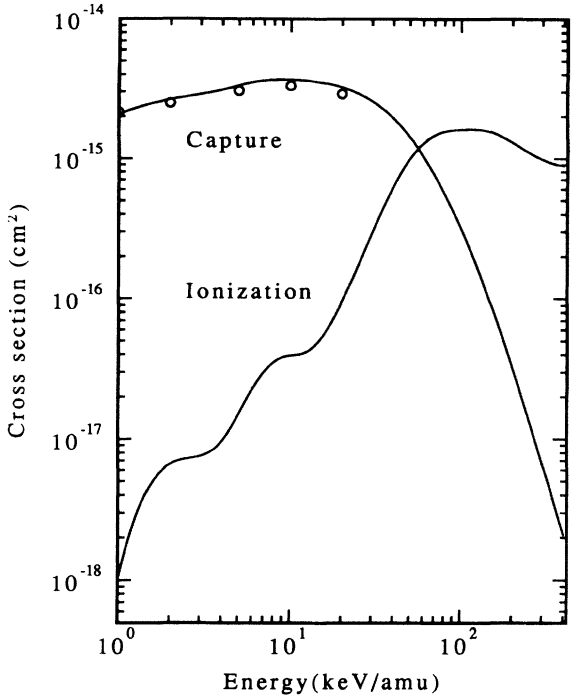

FIG. 4. The same as Fig. 3 but for B^{5+} + H(1s).

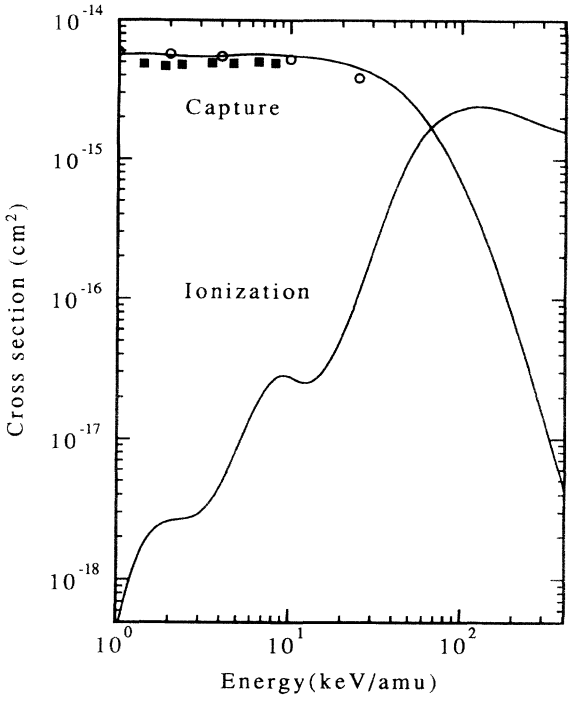

FIG. 6. The same as Fig. 5 but for N^{7+} + H(1s).

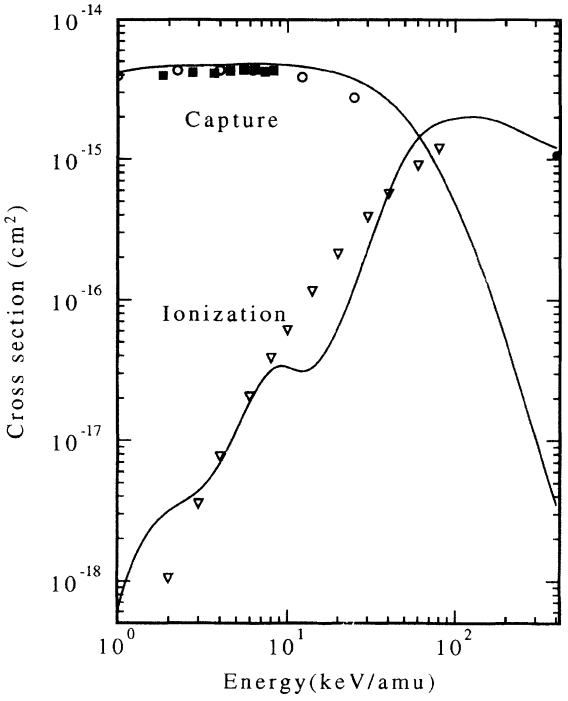

FIG. 5. The ionization and the electron capture cross sections for C^{6+} + H(1s). The open circles are the close-coupling calculations of Fritsch and Lin [8]. The inverted triangles are the ionization cross sections by the adiabatic superpromotion model of Janev *et al.* [9]. The solid squares are the experimental capture cross sections of Meyer *et al.* [15] and the solid circle is the experimental ionization cross section of Shah and Gilbody [3].

= 25 keV/amu. The ionization cross sections of the adiabatic superpromotion model [9] show similar energy dependence as the present results, though the former does not show the humped structure. We tried to resolve the cause of the humped structure but could not elucidate it definitely. Excitation cross sections of the hydrogen

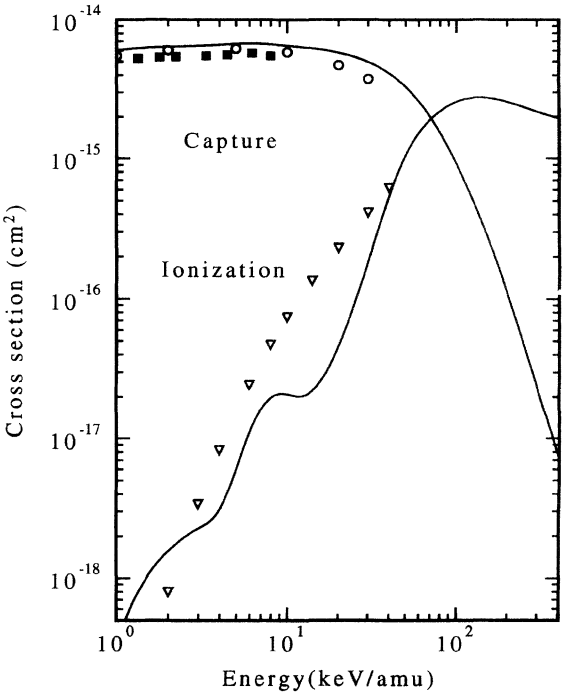

FIG. 7. The same as Fig. 5 but for O^{8+} + H(1s).

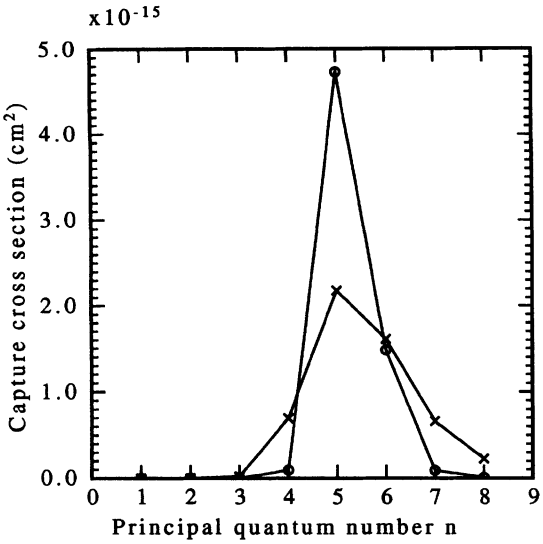

FIG. 8. Partial electron capture cross sections for O^{8+} + H $\rightarrow$ $O^{7+}(n) + p$. The line connecting the open circles is for E = 2 keV/amu and that connecting the crosses is for E = 25 keV/amu.

atom also show the structures at the same energies as shown in Fig. 9. We do not attribute the structures to the instability of the numerical calculations since similar structures were reported in the independent calculations [7,16].

The ionization cross sections and the total electron

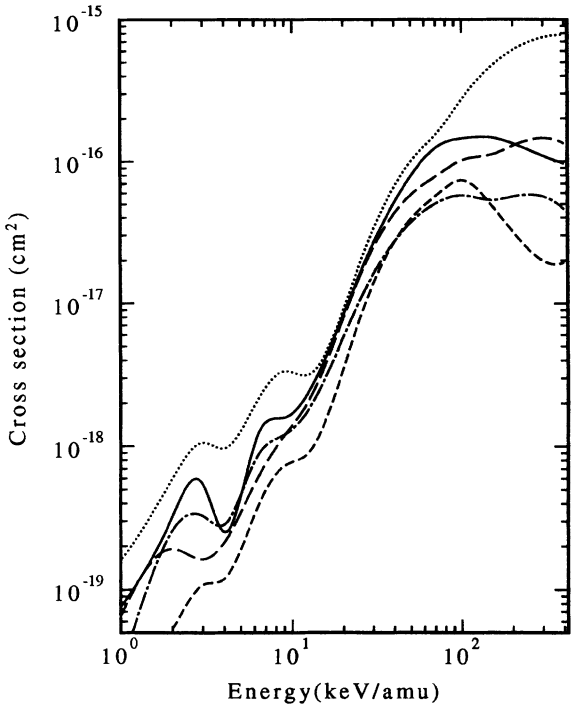

FIG. 9. The excitation cross sections of the hydrogen atom to the states, 2s (solid line), 2p (dotted line), 3s (short-dashed line), 3p (long-dashed line), and 3d (dot-dashed line) for O^{8+} + H.

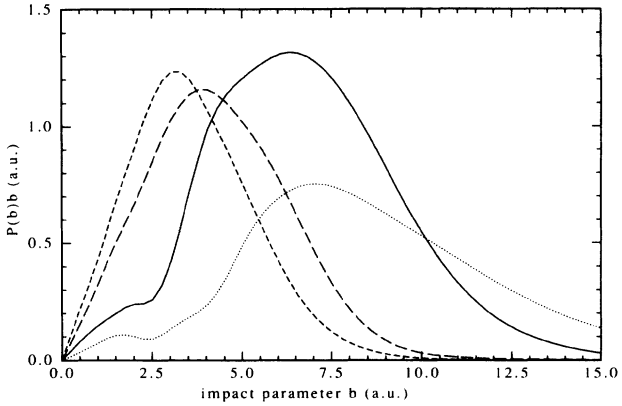

FIG. 10. The impact-parameter (in atomic units) dependence of the transition probabilities of the process O^{8+} + H(1s) at 100 keV/amu. Solid line: ionization to the target continuum; long-dashed line: ionization to the projectile continuum; dotted line: excitation to the target bound states (n=2 - 4); short-dashed line: electron capture to the target bound states.

capture cross sections are summarized in Tables IX and X. Above 50 keV/amu the ionization cross section increase monotonically as the projectile charge Z increases, while it takes the maximum value at B^{5+} below 25 keV/amu. On the other hand, the electron capture cross section in general increases for increasing charge Z with an exception of the interchange of the order within Be^{4+} and B^{5+} below 4 keV/amu.

The contribution of the projectile continuum to the ionization is generally smaller than that of the target continuum. They show different dependence on the impact parameter b. Figures 10 and 11 gives the impact parameter dependence of the transition probabilities of excitation, ionization to the target continuum, electron capture, and ionization to the projectile continuum separately for the process O^{8+} + H(1s). The impact-parameter dependence of the ionization to the target

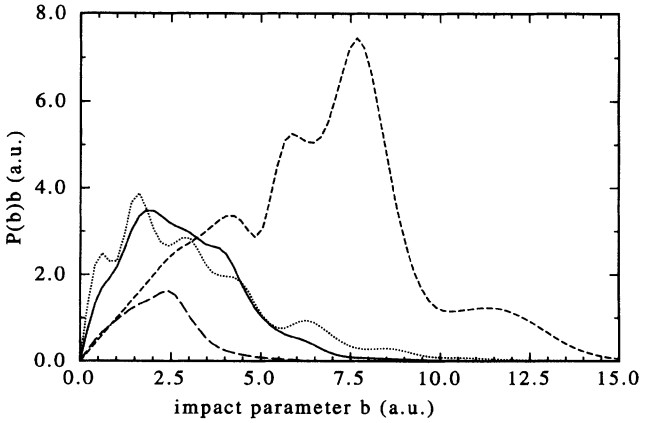

FIG. 11. The same as Fig. 9 but for 4 keV/amu. The ionization and the excitation probabilities are multiplied by a factor of 1000.

TABLE IX. Ionization cross sections (cm^2) for $A^{Z+} + H(1s)$. The numbers in brackets denote the powers of ten to be multiplied.

E (keV/amu)	He^{2+}	Li^{3+}	Be^{4+}	B^{5+}	C^{6+}	N^{7+}	O^{8+}
1.0	2.43[-20]	6.29[-20]	3.96[-19]	1.01[-18]	5.98[-19]	3.90[-19]	3.33[-19]
2.0	3.51[-19]		2.45[-18]	6.60[-18]	3.14[-18]	2.58[-18]	1.55[-18]
3.0		1.32[-18]			4.38[-18]	2.93[-18]	2.26[-18]
4.0			6.27[-18]	9.56[-18]	6.86[-18]	4.64[-18]	3.06[-18]
5.0		6.12[-18]					
6.25			1.76[-17]	2.45[-17]	2.05[-17]	1.59[-17]	1.23[-17]
7.0	8.02[-18]						
9.0			2.28[-17]	3.83[-17]	3.38[-17]	2.83[-17]	2.10[-17]
10.0	1.30[-17]	1.70[-17]					
12.5			2.47[-17]	4.18[-17]	3.10[-17]	2.52[-17]	2.03[-17]
15.0	2.78[-17]						
20.0	6.06[-17]						
25.0	1.19[-16]	1.12[-16]	1.37[-16]	1.73[-16]	1.24[-16]	1.06[-16]	9.43[-17]
30.0	1.91[-16]						
50.0	4.28[-16]	5.95[-16]	7.79[-16]	9.90[-16]	1.03[-15]	1.04[-15]	1.06[-15]
63.0	4.83[-16]						
75.0	4.83[-16]	8.13[-16]	1.12[-15]	1.52[-15]	1.76[-15]	1.94[-15]	2.07[-15]
100.0	4.54[-16]	8.11[-16]	1.22[-15]	1.61[-15]	1.96[-15]	2.31[-15]	2.57[-15]
150.0	3.57[-16]	7.21[-16]	1.08[-15]	1.55[-15]	1.98[-15]	2.37[-15]	2.74[-15]
200.0	3.04[-16]	5.84[-16]	9.33[-16]	1.30[-15]	1.77[-15]	2.15[-15]	2.56[-15]
400.0	1.62[-16]	3.57[-16]	5.98[-16]	8.88[-16]	1.21[-15]	1.59[-15]	1.96[-15]

continuum has a resemblance to that of the excitation regardless of the collision energy, while the ionization to the projectile continuum shows rather different behavior from that of the electron capture at low energies.

In conclusion, we have demonstrated that the close-coupling method based on the pseudocontinuum states expansion gives ionization cross sections of atomic hydrogen systematically in good agreement with experimental data for various projectile charges in a wide energy range, covering from the adiabatic transition region to the perturbative high-energy region. Simultaneously the present calculations produced highly reliable cross sections for excitation and electron capture of the related processes, some of which will be presented in a separate publication since the data such as the state-selected capture cross sections are too vast to be shown in a single paper.

TABLE X. Electron capture cross sections (cm^2) for $A^{Z+} + H(1s)$. The numbers in brackets denote the powers of ten to be multiplied.

E (keV/amu)	He^{2+}	Li^{3+}	Be^{4+}	B^{5+}	C^{6+}	N^{7+}	O^{8+}
1.0	2.56[-16]	2.67[-16]	3.74[-15]	2.06[-15]	4.13[-15]	5.62[-15]	6.06[-15]
2.0	6.37[-16]		3.76[-15]	2.64[-15]	4.61[-15]	5.59[-15]	6.41[-15]
3.0		7.32[-16]			4.65[-15]	5.49[-15]	6.52[-15]
4.0			3.39[-15]	3.10[-15]	4.70[-15]	5.55[-15]	6.63[-15]
5.0		1.18[-15]					
6.25			3.27[-15]	3.55[-15]	4.81[-15]	5.72[-15]	6.77[-15]
7.0	1.28[-15]						
9.0			3.11[-15]	3.68[-15]	4.75[-15]	5.64[-15]	6.61[-15]
10.0	1.33[-15]	1.81[-15]					
12.5			2.97[-15]	3.62[-15]	4.58[-15]	5.45[-15]	6.35[-15]
15.0	1.29[-15]						
20.0	1.16[-15]						
25.0	9.98[-16]	1.68[-15]	2.37[-15]	2.92[-15]	3.74[-15]	4.56[-15]	5.40[-15]
30.0	8.34[-16]						
50.0	3.62[-16]	7.67[-16]	1.13[-15]	1.43[-15]	1.99[-15]	2.61[-15]	3.27[-15]
63.0	2.08[-16]						
75.0	1.31[-16]	3.13[-16]	4.94[-16]	6.51[-16]	9.60[-16]	1.32[-15]	1.73[-15]
100.0	5.59[-17]	1.40[-16]	2.33[-16]	3.20[-16]	4.81[-16]	6.75[-16]	9.10[-16]
150.0	1.31[-17]	3.13[-17]	6.43[-17]	9.17[-17]	1.45[-16]	2.10[-16]	2.92[-16]
200.0	4.39[-18]	1.05[-17]	2.17[-17]	3.28[-17]	5.13[-17]	7.52[-17]	1.08[-16]
400.0	2.52[-19]	5.58[-19]	1.17[-18]	2.08[-18]	3.48[-18]	4.34[-18]	7.46[-18]

ACKNOWLEDGMENTS

The author acknowledges useful comments from Professor H. Tawara. Part of this work has been performed under the collaboration program of National Institute for Fusion Science. This work is also supported by a Grant-in-aid for Scientific Research on Priority Area "Atomic Physics of Multiplycharged Ions" from the Ministry of Education, Science and Culture of Japan.

[1] N. Toshima and J. Eichler, Phys. Rev. Lett. **66**, 1050 (1991); Phys. Rev. A **46**, 2564 (1992).
[2] N. Toshima, J. Phys. B **26**, L281 (1993).
[3] M. B. Shah and H. B. Gilbody, J. Phys. B **16**, L449 (1983).
[4] R. Shakeshaft, Phys. Rev. A **18**, 1930 (1978); R. Shingal and C. D. Lin, J. Phys. B **22**, L445 (1989), N. Toshima, Phys. Lett. A **175**, 133 (1993).
[5] T. G. Winter, Phys. Rev. A **37**, 4656 (1988).
[6] N. Toshima, J. Phys. B **27**, L49 (1994).
[7] W. Fritsch, in *The Physics of Highly Charged Ions*, edited by P. Richard, M. Stockli, C. L. Cocke, and C. D. Lin, AIP Conf. Proc. No. 274 (AIP, New York, 1993), p. 24.
[8] W. Fritsch and C. D. Lin, Phys. Rev. A **29**, 3039 (1984).
[9] R. K. Janev, G. Ivanovski, and E. A. Solov'ev, Phys. Rev. A **49**, 645 (1994).
[10] M. B. Shah and H. B. Gilbody, J. Phys. B **14**, 2361 (1981).
[11] M. B. Shah, D. S. Elliott, P. McCallion, and H. B. Gilbody, J. Phys. B **21**, 2455 (1988).
[12] N. Toshima, J. Phys. B **25**, L635 (1992).
[13] W. Fritsch and C. D. Lin, J. Phys. B **15**, L281 (1982).
[14] M. B. Shah and H. B. Gilbody, J. Phys. B **15**, 413 (1982).
[15] F. W. Meyer, A. M. Howald, C. C. Havener, and R. A. Phaneuf, Phys. Rev. A **32**, 3310 (1985).
[16] W. Fritsch, R. Shingal, and C. D. Lin, Phys. Rev. A **44**, 5686 (1991).